

PAPER • OPEN ACCESS

Investigation of plasma states formed under the interaction of high-power laser pulses with wire-shape Al–Cu target

To cite this article: D O Golovin *et al* 2021 *J. Phys.: Conf. Ser.* **1787** 012028

View the [article online](#) for updates and enhancements.

A promotional banner for the 240th ECS Meeting. The banner features a colorful striped border at the top. On the left, the ECS logo is displayed in a green circle. To its right, the text reads "240th ECS Meeting" in large blue font, followed by "Digital Meeting, Oct 10-14, 2021" in a smaller blue font. Below this, it says "Register early and save up to 20% on registration costs" in bold black font, and "Early registration deadline Sep 13" in a smaller black font. At the bottom left, there is a red "REGISTER NOW" button. On the right side of the banner, there is a photograph of a diverse group of people in professional attire, smiling and clapping, suggesting a successful event or meeting.

ECS **240th ECS Meeting**
Digital Meeting, Oct 10-14, 2021
**Register early and save
up to 20% on registration costs**
Early registration deadline Sep 13
REGISTER NOW

Investigation of plasma states formed under the interaction of high-power laser pulses with wire-shape Al–Cu target

D O Golovin¹, M A Alkhimova^{2,3}, T A Pikuz^{1,4,6}, Y Abe¹, Y Honoki¹, S Lee¹, K Matsuo¹, K Koga¹, K Okamoto¹, S Shokita¹, Y Arikawa¹, A Ya Faenov^{1,4}, S Fujioka¹, S A Pikuz^{3,2}, I Yu Skobelev^{3,2}, H Nishimura¹ and A Yogo^{1,5}

¹ Institute of Laser Engineering, Osaka University, 2-6 Yamadaoka, Suita, Osaka 565-0871, Japan

² National Research Nuclear University MEPhI (Moscow Engineering Physics Institute), Kashirskoe Shosse 31, Moscow 115409, Russia

³ Joint Institute for High Temperatures of the Russian Academy of Sciences, Izhorskaya 13 Bldg 2, Moscow 125412, Russia

⁴ Graduate School of Engineering, Osaka University, 2-1 Yamadaoka, Suita, Osaka 565-0871, Japan

⁵ Precursory Research for Embryonic Science and Technology, Japan Science and Technology Agency, Honcho 4-1-8, Kawaguchi, Saitama 332-0012, Japan

⁶ Kansai Photon Science Institute, National Institutes for Quantum and Radiological Science and Technology, 8-1-7 Umemidai, Kizugawa-shi, Kyoto 619-0215, Japan

E-mail: golovin-d@ile.osaka-u.ac.jp

Abstract. Study of warm dense matter remains a very important task for understanding of many unique phenomena observing as in astrophysical research as in inertial fusion and fast ignition. In this work, we studied the parameters of plasma created by 1.7 ps laser pulses of relativistic intensity of 7×10^{18} W/cm² in a specially designed Al–Cu wire-shape target, in comparison with a flat Cu and Al foil targets. We observed the strong emission of neutral or virtually neutral Cu K_α line from both Cu foil and Cu wire part of targets, which indicates the creation of a dense state exposed to the intense flow of hot electrons. Parameters of the plasma were evaluated by comparison of experimental spectra with the results of modeling by collisional-radiative kinetic code PrismSpec under the plasma zone approach. The using of Al foil in front of Cu wire part of target allowed avoiding the direct heating of Cu-wire and acquiring spectra of Cu K-shell emission evidently belonging to emission of warm dense matter (WDM) state. The upper estimate for the electron temperature in WDM region was found to be below 80 eV.

1. Introduction

Accurate and comprehensive studies of dense matter at extreme states are very important as for understanding the unique astrophysical phenomenon and its following modeling in experiments in laboratory conditions [1, 2], as for studying peculiarities appearing in inertial confinement fusion research [3]. Estimation of the parameters like electron temperature and density allows defining conditions and regime of heating of the plasma. One of the mostly challenging states



of matter to be determined and investigated experimentally is warm dense matter (WDM). This matter states corresponds to the plasma with near solid or solid density heated up to the electron temperature of several to tens eV [4]. The WDM could be achieved in some plasma regions formed during laser–target interaction when these regions are relatively outlying from the interaction region where the main part of laser energy is absorbed [5]. However, the description of physical processes remains very complicated due to strong interaction between particles [6].

In general, the radiative diagnostics of WDM state is complicated because of its low emissivity compare to the emissivity of hot plasma created in the region directly heated by the laser. For example, in [7], by means of x-ray spectroscopy with spatial resolution the parameters of WDM isohorically heated by hot electron flow only had been evidently measured. The emission spectrum of neutral K_α and its cold satellites was under consideration. It is well established that interaction between the picosecond laser pulse and thin (μm thick) foil creates a big number of hot electrons. Electrons with energy, not enough to escape the target, recirculating inside the target plasma, enhancing strong sheath field which leads to more efficient ion acceleration [8]. On the other hand, electrons with the highest energy are able to escape the foil. Then a wire, attached on a rear side of the foil, may guide those electrons and magnetic field around it. If the incoming electron kinetic energy is enough to ionize inner shell electrons in the guiding material, which remains in the solid density state, the characteristic K-shell radiation is emitted. This emission can be used as diagnostic instrument.

One of the approaches for investigating WDM in experiments with laser-produced plasma is an application of wire-shaped targets [4, 7]. Several types of wire targets were used to study hot electrons propagation [9, 10]. The guiding of electrons along the metallic wire under the balance of electric and magnetic fields, surrounding the wire, was theoretically predicted [11] and observed experimentally [12, 13].

The effect of K-shell emission from the copper wire, attached on the rear side of aluminum foil, was observed at LFEX [14] laser experiments. At that experiments the ps-laser pulse with an intensity of $\sim 10^{19}$ W/cm² irradiated 10 μm Al foil with a backside attached complex wire-shape structure. As a result of the efficient high energy electrons production inside the foil, relatively strong K_α emission was generated practically in all volume of copper. The sketch of the target and the pattern of K_α radiation measured by means of K_α imager technique [3] are shown in figure 1. In the pattern (on left) it is seen that K_α signal is stronger where the parts of the target are closer to the focal spot (red dot in the sketch), while some radiation also comes from the wire part of the target. It is also can be seen that the shape of the volume, from which K_α is emitted, closely corresponds to the shape of the target. It means that at the time of K_α emission the target was not significantly expanded. In addition, the Al foil was not only the source of hot electrons but also the source of protons, accelerated in direction normal to the target by target normal sheath acceleration (TNSA) mechanism. This proton beam was used as a probe for the radiography of electrical and magnetic fields created around the target. Although the detailed discussion on proton radiography results is beyond the scope of current paper, we would like to notice that those contain some specific feature in the distribution of deviated protons, which could be attributed to the influence of encircle magnetic field caused by electron motion, induced in the wire. The formation of such encircle magnetic field gave an evidence of correctness of the theoretical prediction and numerical simulations [11]. In perspective, by attaching the second wire to the first one it will be possible to model a magnetic reconnection effect with a reconnection point in the region between two wires. This task is a hot topic in research with an astrophysical relevance [15].

Experimental confirmation of the generation of encircle magnetic field in the wire and further investigations of the mechanism of magnetic field generation in described experiments require to have comprehensive data about target heating, energy transport, particle energy distribution and emission properties of the plasma. In particular, it is important to measure

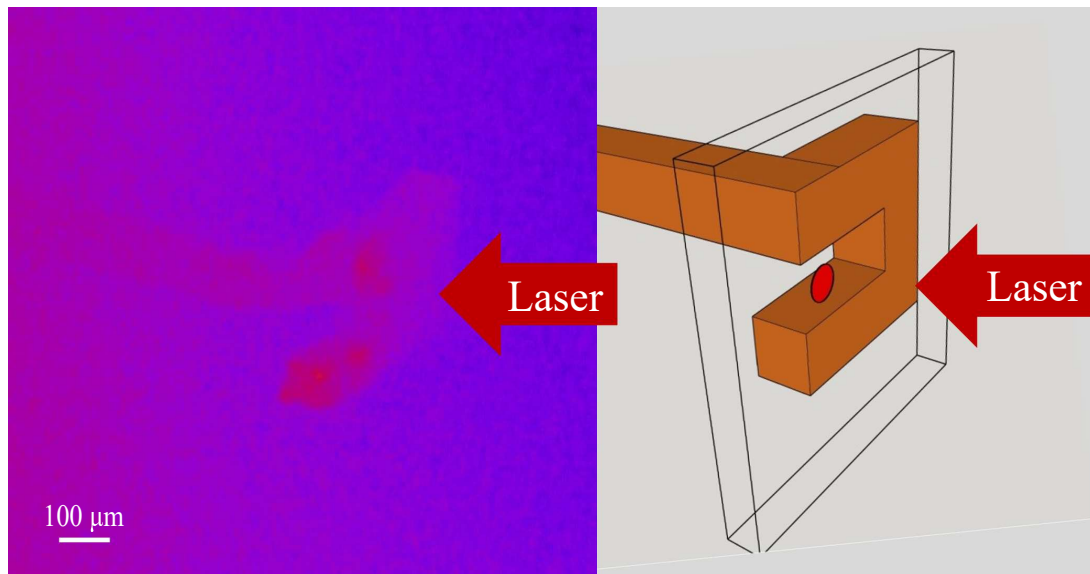


Figure 1. Image from K_{α} -imager (left): magnification is $20\times$, spatial resolution is $13\ \mu\text{m}$ and spectral bandwidth is $5\ \text{eV}$ [3]. Sketch of the target with point of laser irradiation (right): aluminum foil is shown transparent.

the electron temperature, the electron density and ionization state of matter created during laser–target interaction. For that an x-ray spectroscopy is one of commonly used and powerful diagnostic approach. In this article spectroscopic measurement presented for the test-case of laser interaction with flat Cu target and for the cases of using Al–Cu wire-shape targets with and without wire. Parameters of plasma obtained by comparison of experimental spectra with the result of kinetic modeling by collisional-radiative spectral analysis code PrismSpect [16] are under discussion.

2. Experiment

Experiment was done at the LFEX laser facility operated in the ILE, Osaka University, Japan. We used two simultaneously delivered LFEX laser beams focused in one spot with a total energy of $490\ \text{J}$ on target within pulse duration of $1.7\ \text{ps}$. Laser beams were focused by two $f/10$ off-axis parabolas in the focus spot about $60\ \mu\text{m}$ on full width at half maximum (FWHM) which corresponds to the peak intensity about $7 \times 10^{18}\ \text{W}/\text{cm}^2$. The contrast ratio of the laser pulse peak and the prepulse at $200\ \text{ps}$ before the main peak was estimated to be 10^{10} [17]. Experimental setup and target configurations are schematically shown in figure 2. Laser pulse was directed to the front side of the target at the angle 41.8° to its normal. X-ray emission spectra were measured by two focusing x-ray spectrometers with high spatial resolution (FSSRs) [18] with spherically bent crystals. The crystals provided high luminosity and the spectral resolution about $\lambda/\Delta\lambda \approx 3000$.

The first spectrometer, FSSR-F was equipped with alpha-quartz ($[2\bar{2}43]$) crystal with lattice spacing $2d = 2.024\ \text{\AA}$ and was aligned to measure Cu K-shell x-ray emission at the wavelength range $\Delta\lambda = 1.3\text{--}1.7\ \text{\AA}$ in the first reflection order.

The second spectrometer at the rear of the target, FSSR-R, was equipped with mica crystal with $2d = 19.94\ \text{\AA}$ lattice spacing allowing to observe K-shell emission of both Al and Cu ions in II and VIII reflection orders correspondingly. To reduce the contribution from the first order of reflection the $25\ \mu\text{m}$ thick polypropylene filter was placed in front of the crystal.

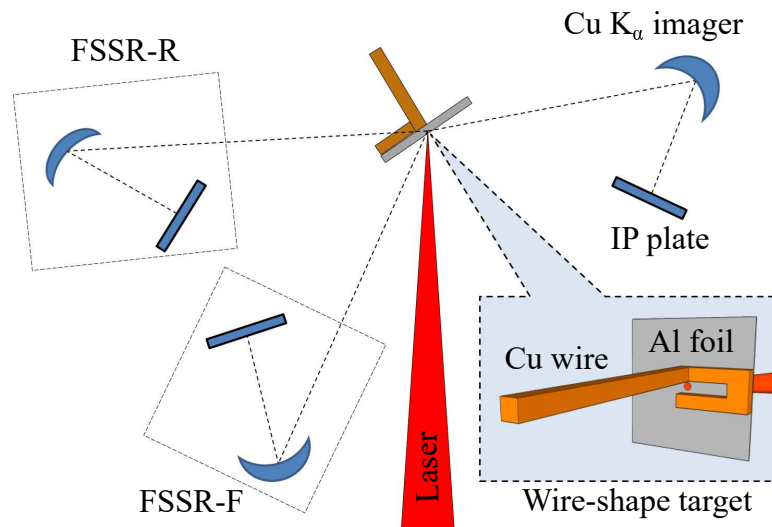


Figure 2. Configurations of experimental setup and targets: inset shows back side view of the Al–Cu wire-type target(right bottom); the red points indicate the position of laser focus.

The crystal was aligned to work in VIII order of reflection to detect the signal from K-shell emission of Cu ions (lines He_α with $\lambda_{\text{He}_{\alpha 1}} = 1.477 \text{ \AA}$ and $\lambda_{\text{He}_{\alpha 2}} = 1.485 \text{ \AA}$, and K_α doublet with $\lambda_{\text{K}_{\alpha 1}} = 1.5406 \text{ \AA}$ and $\lambda_{\text{K}_{\alpha 2}} = 1.5444 \text{ \AA}$) in the wavelength range of $\delta\lambda^{\text{VIII}} = 1.4\text{--}1.9 \text{ \AA}$. Simultaneously, in the II order of reflection the spectra containing lines of Al K-shell emission ($\lambda_{\text{Ly}_\beta} = 6.05 \text{ \AA}$, $\lambda_{\text{He}_\beta} = 6.635 \text{ \AA}$, $\lambda_{\text{Ly}_\alpha} = 7.17 \text{ \AA}$) were measured in the wavelength range of $\delta\lambda^{\text{II}} = 5.6$ to 7.6 \AA [19].

Measured time-integrated spectra were exposed on BAS-TR2040 image plates (IP). After exposure, IPs were scanned using absolutely calibrated Typhoon FLA 7000 scanner [20] with spatial resolution of $25 \mu\text{m}$. To protect the IP against visible light, the windows of IP holders were covered by $22 \mu\text{m}$ Al foil and 2 layers of (C_6H_6 $2 \mu\text{m}$ + Al $0.2 \mu\text{m}$) filter for spectrometer with quartz and mica crystal, correspondingly.

3. Result and discussion

Initially a simple flat Cu foil was examined as a reference target. Target had thickness of $5 \mu\text{m}$ and a size of $1 \times 1 \text{ mm}^2$. The data taken by FSSR-F spectrometer are given in figure 3(a). The measured x-ray emission spectrum appears to be complex containing several group of lines belonging to the different ionic charge states. Particularly, the appearance of He-like Cu XXVIII resonance transitions ($\lambda_{\text{He}_{\alpha 1}} = 1.477 \text{ \AA}$ and $\lambda_{\text{He}_{\alpha 2}} = 1.485 \text{ \AA}$) indicates that plasma reached high ionization states and the temperature is significantly above 1 keV. At the same time the presence of K_α and K_β lines ($\lambda_{\text{K}_\beta} = 1.392 \text{ \AA}$, $\lambda_{\text{K}_\alpha} = 1.54 \text{ \AA}$) points out to the contribution of a cold plasma region exposed to a fast electron flow. Indeed, a simulation of spectral emissivity for such plasma is rather complicated.

Kinetic modeling of the measured spectrum was carried out using the PrismSpect collisional-radiative computational code at the steady state approximation [16]. At first it was found that x-ray yield in the spectral range of the He_α line can be well fit if to imply the electron density $N_{e1} = 1 \times 10^{21} \text{ cm}^{-3}$ and the electron temperature $T_{e1} = 3000 \text{ eV}$, while the 0.1% fraction of hot electrons with the temperature of $T_{\text{hot}} = 10 \text{ keV}$ was included in the modeling. The simulated intensity profile is shown in red in figure 3(b). At once, it is clearly seen that the

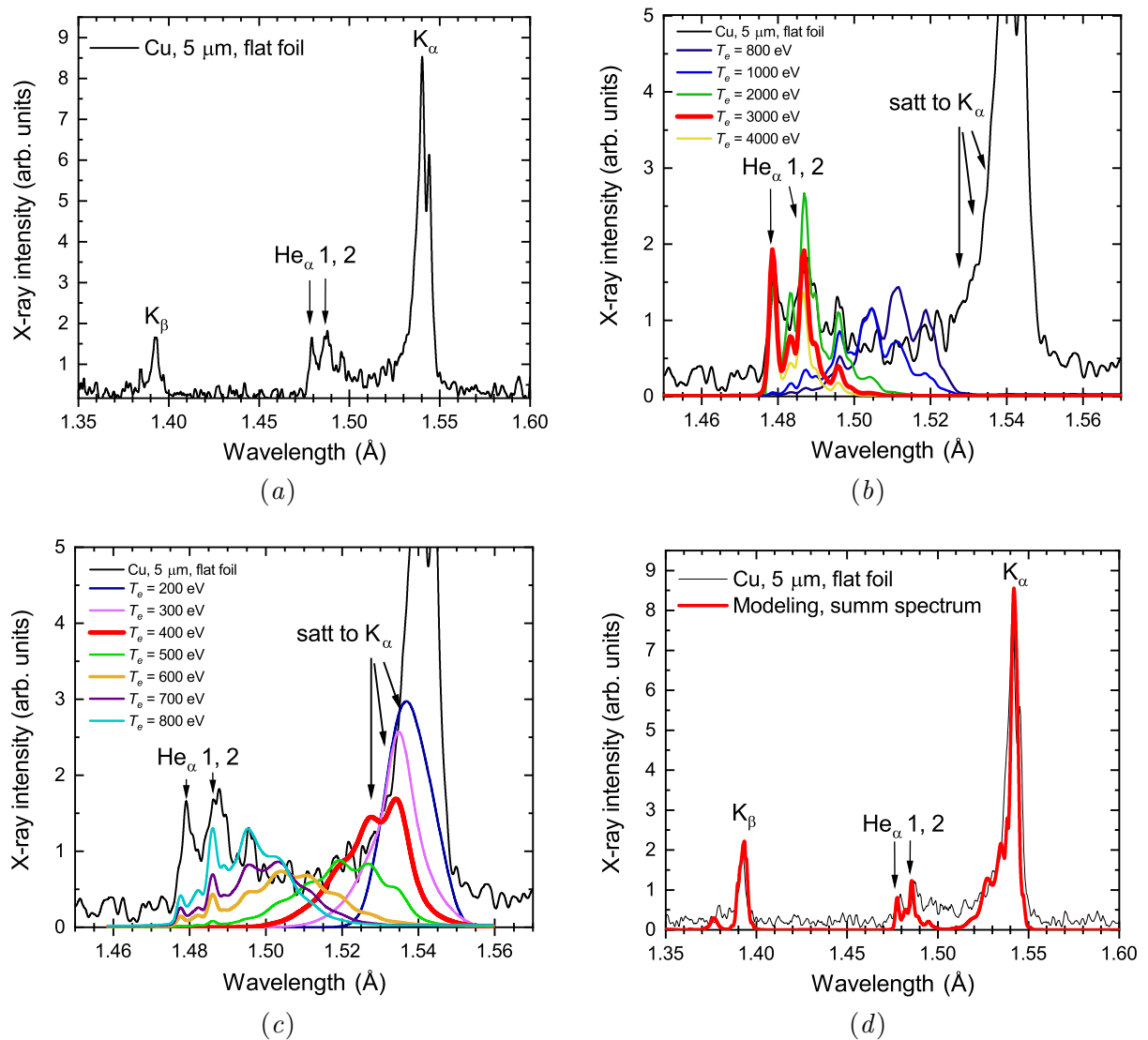


Figure 3. (a) X-ray spectrum, measured by FSSR-F for reference Cu 5 μm flat foil target; (b) evaluation of electron temperatures for Cu zone 1 corresponding to the focal spot region with $N_e = 1 \times 10^{21} \text{ cm}^{-3}$; (c) evaluation of electron temperatures for Cu zone 2 corresponding to peripheral plasma region with $N_i = N_{\text{solid}} = 8.2 \times 10^{22} \text{ cm}^{-3}$; (d) comparison of experimental spectrum with the sum spectrum modeled by plasma zones conception. In all panels the experimental spectrum is shown in black.

modeling successfully describes only a small part of the experimental spectrum. Thus, the actual experimental conditions could not be described by a plasma with only one set of parameters averaged on time and space. Aside of the contribution from the hottest area emitting He-like lines one should obviously consider the emission from a peripheral areas and later stages of plasma evolution also.

To complete the modeling of our multicomponent spectrum, we perform simulation using the approach, previously developed in [21–25]. There the plasma is considered to consist of several regions, namely plasma zones, heated up by different mechanisms. The differentiation of the total plasma volume into separate zones is shown schematically in figure 4(a). However, in real

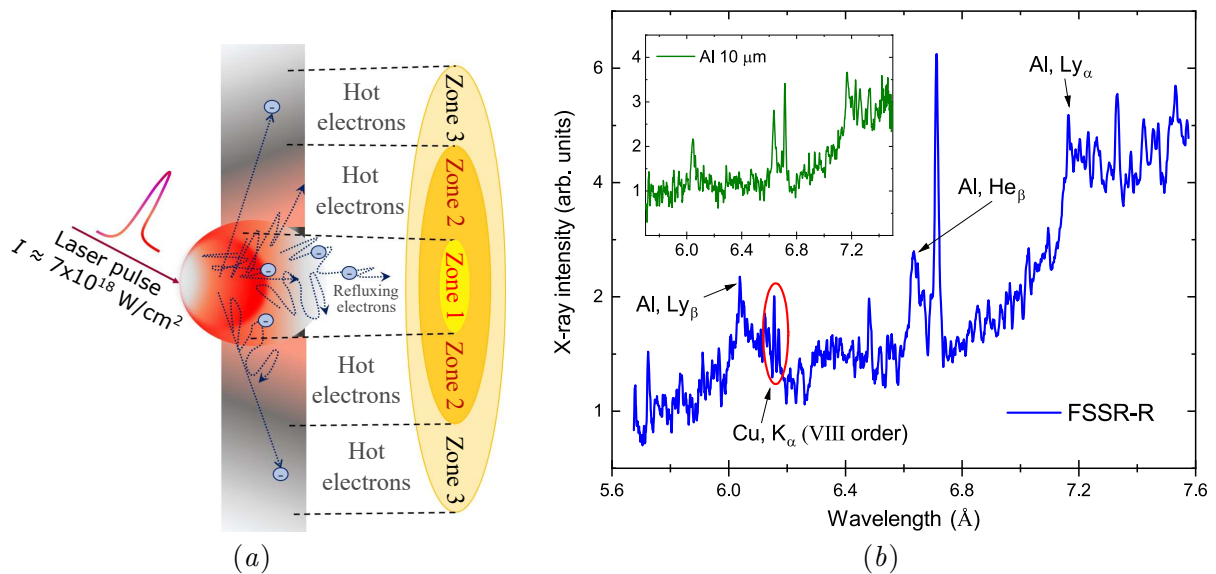


Figure 4. (a) Schematic diagram of plasma differentiation in the zone concept used for modeling spectral emission from flat Cu target. (b) Experimental spectra measured from pedestal-shape target. The main panel shows the Al spectrum recorded by FSSR-R spectrometer in the II reflection order. The rise of intensity in the right wing of Ly_{β} due to Cu K_{α} emission from VIII order of reflection is marked by red oval. Spectrum of Al foil 10 μm thickness recorded by FSSR-F during another shot is presented in the inserted panel.

plasma a clear spatial allocation of individual zones appears as conditional. With a significant degree of certainty, the first zone can be defined as the zone in which the target is directly heated by a laser pulse. Other zones are peripheral and reflect the efficiency of secondary processes transferring the energy from the hottest zone via conductivity by bulk thermalized electrons in the nearest vicinity and by relativistic electron flow at distant area. In fact, in most cases that processes occur on the spatial scale which cannot be resolved by existing experimental methods.

According with the plasma zone concept the modeling result given in figure 3(b) corresponds to the contribution from the most ionized zone 1 heated up to 3000 keV temperature. Presumably zone 1 is directly heated by the laser pulse and has a size approximately equal to the diameter of focal spot of 60 μm .

Obviously, the rest part of the spectra is emitted by colder plasma regions. One can see two important features in the spectrum. The first is the presence of group of satellites located on the short wavelength wing of Cu K_{α} line. The variation of the plasma temperature, with the assumption that peripheral parts of target remains solid of ion density $N_i \approx 8.2 \times 10^{22} \text{ cm}^{-3}$, allowed to describe the part of the spectrum in the range of 1.51–1.53 \AA . The best agreement with the measured spectra in the range was reached at $T_{e2} = 400 \text{ eV}$ [red profile in figure 3(c)]. In turn, the second feature is in the presence of quite strong emission of neutral K_{α} and K_{β} lines, which points out on the existence of a plasma region being below 100 eV temperatures but exposed to hot electron flow [peripheral zone 3 in figure 4(a)]. The red curve in figure 3(d) shows the final comparison of the reference spectrum from flat Cu foil with the result of modeling presented as a sum of the best fitting spectra obtained for different plasma zones.

To underline, the analysis of neutral K_{α} line profile is a powerful instrument to reveal the parameters of such an isochorically heated warm dense matter [26, 27]. However, it is always an issue how to discriminate the spectral contribution emitted by WDM far vicinity from that

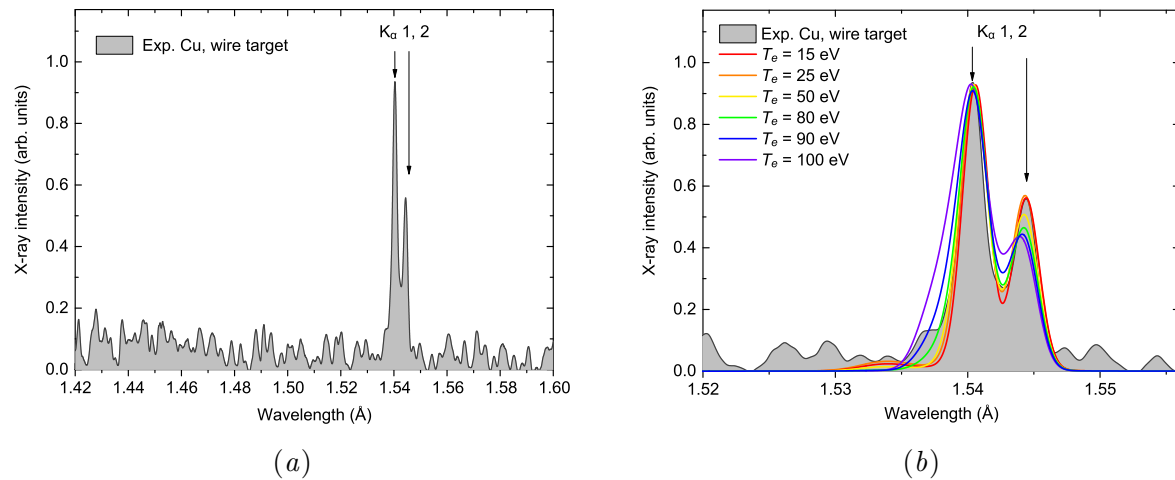


Figure 5. (a) Spectrum of wire-shape target measured using FSSR-R spectrometer equipped with mica crystal in VIII order of reflection. (b) Comparison of experimental spectrum with modeling results.

manifold brighter emission coming from a hotter plasma zone. In the particular spectra of the flat Cu foil, the overlapping of the emission from zones 2 and 3 evidently makes the measurement of T_e in zone 3 impossible.

To mitigate the issue here we propose to implement the targets made of two different atomic elements where the first will be exposed to the laser impact and the second, being placed at the rear side of the target, will be heated up by secondary processes only.

To implement the idea the target schematically shown in the right-side bottom inset in figure 2 was chosen. At the back of 10 μm Al foil the copper wire was attached having $100 \times 100 \mu\text{m}^2$ square cross-section, the pedestal arc (or yoke) with 100 μm central gap, and 1600 μm long standing tip. The laser was focused on the Al surface to the point located in the middle of the yoke gap.

Spectral data measured by FSSR-R spectrometer is shown in figure 4(b) and recorded in II and VIII orders of reflection of mica crystal. Obtained spectrum contains of Ly_{α} line emitted by H-like aluminum ions confirming the plasma is highly ionized. In turn, hot electrons effectively accelerated on the front surface of the target, propagated deep into Al and Cu layers and did initiate an intense bremsstrahlung radiation together with a neutral Cu K_{α} emission. Though Cu K_{α} ($\lambda_{K_{\alpha}} = 1.54 \text{ \AA}$) relative intensity appeared to be weak, it was reflected by VIII order of the crystal being 3 times less reflective than the II order delivering Al emission. For the reference one may also note the spectrum obtained for a pure Al target containing no spectral feature in the range of Cu K_{α} line appearance.

Figure 5(a) represents the spectrum obtained by FSSR-F spectrometer equipped with quartz crystal and not suitable to register Al K-shell emission. The spectrum has significant distinctions compare to the flat foil case [see figure 3(a)], as there are no spectral components emitted by a highly charged (H-, He-, Li-like) Cu ions but Cu K_{α} line only. It confirms the direct heating of the copper matter by the laser was avoided, and the Cu spectra can be analyzed as being fully belong to a peripheral area heated by hot electron flow. Another evidence of the wire heating is the x-ray image shown in figure 1, where the signal came not only from copper pedestal but also from the wire itself. Since K_{α} photons mean free pass in copper is 15 μm [28] it is possible that high intense K_{α} emission is generated when the electrons propagate on the surface of the wire, as it was described in [10, 11]. In figure 5(b), the spectra measured in

the case of the wire-shape target are compared with the results of kinetic modeling in the K_α spectral region. Under reasonable assumption the ion plasma density to be of the solid state one $N_i = N_{\text{solid}} = 8.2 \times 10^{22} \text{ cm}^{-3}$, we varied the electron temperature to find the best match in the profile of K_α doublet. The temperature appears to be not so high to modify the profile of the line significantly. Paying the attention to the short-wavelength wing of the line, we can conclude the observed line is narrower than for the cases of 90 and 100 eV in the modeling. Accordingly, the outcome is the upper-limit estimate for the electron temperature in the wire and yoke pedestal (all representing zone 3) to be of $T_e \leq 80 \text{ eV}$. In the same time, one should expect less effective heating and lower temperatures about 10–30 eV. The sensitivity of the K_α line profile to the lower temperature values directly depends on the number of bound electrons on the outer shell of an ion. So, in order to provide more careful revealing of the temperature in WDM region of the laser irradiated target, the wire (or in general—a periphery of the target) should be manufactured of moderate- Z metals like Ti or V.

Most obviously the heating is caused by hot electron current induced in the solid copper, as it was already well-studied [29–31]. In addition the matter could be heated radiatively by intense x-rays generated in the hot zone. Radiative pumping mechanism might even dominates over collisional processes in ultra-relativistic solid density laser plasma [32,33]. If the case, it leads to a large populations of hollow atoms states to be clearly distinguished due to their x-ray emission in a specific range of K-shell spectra. However, those spectral features are not observed in the spectra and so we conclude the heating of the wire is governed by hot electrons.

4. Conclusion

By means of high-resolution x-ray spectroscopy we investigated the parameters of plasma created by 1.7 ps laser pulses of relativistic intensity of $7 \times 10^{18} \text{ W/cm}^2$ in a specially designed Al–Cu wire-shape targets, in comparison with a flat Cu and Al foil targets. The strong emission of neutral or virtually neutral Cu K_α line is observed from both Cu foil and Cu-wire part, which indicates the creation of a dense state exposed to the intense flow of hot electrons. Parameters of the plasma were evaluated by the comparison of experimental spectra with kinetic modeling results provided under the plasma zone approach. In the case of Cu foil target plasma parameters were determined for the hottest plasma region ($T_{e1} = 3000 \text{ eV}$; $N_{e1} = 1 \times 10^{21} \text{ cm}^{-3}$) and in the hot peripheral zone ($T_{e2} = 400 \text{ eV}$, $N_{e2} = 1.5 \times 10^{24} \text{ cm}^{-3}$). However, it was impossible to reveal the temperature for the further, warm plasma zone, due to the spectral overlapping in the emission from hot and warm zones. To mitigate the issue it is suggested to use a target made of two different materials where the first is exposed to the laser impact and the second, being placed at the rear side of the target, to be heated up by secondary processes only. The concept is realized with a special Al–Cu wire target having its own research attraction in the context of magnetic reconnection studies. By laser irradiation of $10 \mu\text{m}$ Al foil substrate we succeed to avoid the direct heating of Cu wire at the back side of the target. Correspondingly, the acquired spectra of Cu K-shell emission purely belonged to the emission of WDM wire heated by an intense flow of hot electrons.

The profile of the measured Cu K_α line was analyzed with the comparison to the results of atomic kinetics modeling. The upper estimate for the electron temperature in WDM region was found to be below 80 eV. The concept with double-element targets to provide x-ray spectroscopy measurements of laser-generated WDM parameters to be done at full with a proper choice of the peripheral target layer (or of a structure at the back of the target) made of moderate- Z metals.

Acknowledgments

This work was supported by Grants in Aid for Scientific Research (No. 25420911 and 26246043) of the Ministry of Education, Culture, Sports, Science and Technology of Japan (MEXT), Adaptable and Seamless Technology Transfer Program through Target-driven Research and

Development (A-STEP) (No. AS2721002c), the Japan Science and Technology Agency (JST) and the Precursory Research for Embryonic Science and Technology (PRESTO) (JPMJPR15PD). We thank the ILE technical support staff for their assistance with the laser operation, target fabrication and plasma diagnostics. This work was also supported by the ILE, Osaka University (2017A1-YOGO). We also acknowledge financial support from the Ministry of Science and Higher Education of the Russian Federation within state assignment to the JIHT RAS (topic 01201357846).

We are especially grateful to Professor A Zhidkov (Photon Pioneers Center, Osaka University) for theoretical support of this work.

References

- [1] Brandenburg A and Subramanian K 2005 *Phys. Rep.* **417** 1–209
- [2] Golovin D O *et al* 2020 *High Energy Density Phys.* **36** 100840
- [3] Sakata S *et al* 2018 *Nat. Commun.* **9** 3937
- [4] Kress J, Cohen J S, Horner D, Lambert F and Collins L 2010 *Phys. Rev. E* **82** 036404
- [5] Stafford A, Safronova A, Faenov A Ya, Pikuz T, Kodama R, Kantsyrev V, Shrestha I and Shlyaptseva V 2017 *Laser Part. Beams* **35** 92–9
- [6] Renaudin P, Blancard C, Cléroutin J, Faussurier G, Noiret P and Recoules V 2003 *Phys. Rev. Lett.* **91** 075002
- [7] Schönlein A *et al* 2016 *EPL* **114** 45002
- [8] Yogo A *et al* 2017 *Sci. Rep.* **7** 42451
- [9] Wei M, Solodov A, Pasley J, Stephens R, Welch D and Beg F 2008 *Phys. Plasmas* **15** 083101
- [10] Kar S *et al* 2016 *Nat. Commun.* **7** 10792
- [11] Kodama R *et al* 2004 *Nature* **432** 1005
- [12] Quinn K *et al* 2009 *Phys. Rev. Lett.* **102** 194801
- [13] Tokita S, Otani K, Nishoji T, Inoue S, Hashida M and Sakabe S 2011 *Phys. Rev. Lett.* **106** 255001
- [14] Kawanaka J *et al* 2008 *J. Phys.: Conf. Ser.* **112** 032006
- [15] Gu Y J, Pegoraro F, Sasorov P V, Golovin D, Yogo A, Korn G and Bulanov S V 2019 *Sci. Rep.* **9** 1–10
- [16] MacFarlane J J, Golovkin I E, Woodruff P R, Kulkarni S K and Hall I M 2013 Simulation of plasma ionization and spectral properties with PrismSPECT 2013 *Abstracts IEEE Int. Conf. on Plasma Science (ICOPS)* (New York: IEEE)
- [17] Arikawa Y *et al* 2016 *Appl. Opt.* **55** 6850–7
- [18] Faenov A Ya, Pikuz S, Erko A, Bryunetkin B, Dyakin V, Ivanenkov G, Mingaleev A, Pikuz T, Romanova V and Shelkovenko T 1994 *Phys. Scr.* **50** 333
- [19] Alkhimova M A, Skobelev I Yu, Faenov A Ya, Arich D, Pikuz T A and Pikuz S A 2018 *Quantum Electron.* **48** 749
- [20] Williams G J, Maddox B R, Chen H, Kojima S and Millecchia M 2014 *Rev. Sci. Instrum.* **85** 11E604
- [21] Pikuz S A *et al* 2017 *JETP Lett.* **105** 13–7
- [22] Pikuz S A, Faenov A Ya, Fortov V E and Skobelev I Yu 2014 *Phys. Usp.* **57** 702
- [23] Faenov A Ya *et al* 2015 *Sci. Rep.* **5** 13436
- [24] Colgan J *et al* 2013 *Phys. Rev. Lett.* **110** 125001
- [25] Colgan J *et al* 2016 *EPL* **114** 35001
- [26] Hansen S B *et al* 2005 *Phys. Rev. E* **72** 036408
- [27] Nishimura H *et al* 2003 *J. Quant. Spectrosc. Radiat. Transfer* **81** 327–37
- [28] Hubbell J 1999 *Phys. Med. Biol.* **44** R1
- [29] Yoshida M, Fujimoto Y, Hironaka Y, Nakamura K G, Kondo K i, Ohtani M and Tsunemi H 1998 *Appl. Phys. Lett.* **73** 2393–5
- [30] Rathore R, Singhal H and Chakera J 2019 *J. Appl. Phys.* **126** 105706
- [31] Reich C, Gibbon P, Uschmann I and Förster E 2000 *Phys. Rev. Lett.* **84** 4846
- [32] Basko M M 1978 *Astrophys. J.* **223** 268–81
- [33] Emslie A G, Phillips K J H and Dennis B R 1986 *Sol. Phys.* **103** 89–102